



APOE ε4 potentiates tau related reactive astrogliosis assessed by cerebrospinal fluid YKL40 in Alzheimer's disease



Lydia Trudel ^{1,2,3}✉, Joseph Therriault ^{1,3}, Arthur C. Macedo ^{1,3}, Marcel S. Woo ^{1,4,5}, Nesrine Rahmouni ^{1,3}, Étienne Aumont ^{1,3}, Stijn Servaes ¹, Seyyed Ali Hosseini ^{1,3}, João Pedro Ferrari-Souza ^{6,7}, Bruna Bellaver ⁶, Pamela L. Ferreira ⁶, Tevy Chan ^{1,3}, Yi-Ting Wang ^{1,3}, Jaime Fernandez-Arias ^{1,3}, Yansheng Zheng ^{1,3}, Brandon Hall ^{1,3}, Jenna Stevenson ¹, Robert Hopewell ⁸, Chris Hung-Hsin Hsiao ⁸, Maxime Montembeault ¹, Jesse Klostranec ⁹, Yasser Iturria-Medina ³, Paolo Vitali ¹, Thomas K. Karikari ^{10,11,12}, Andrea L. Benedet ⁶, Nicholas J. Ashton ^{10,11,12,13,14}, Eduardo Zimmer ^{7,15,16}, Serge Gauthier ¹, Tharick A. Pascoal ⁶, Henrik Zetterberg ^{10,12,17,18,19,20}, Kaj Blennow ^{10,12,21,22} & Pedro Rosa-Neto ^{1,3,23}✉

Abstract

Background Glial responses are involved in neurodegenerative processes, with tau pathology often associated with increased glial inflammatory responses in Alzheimer's disease (AD). The apolipoprotein E (APOE) ε4 allele, the major genetic susceptibility gene for AD, might contribute to this process by modulating both tau pathology and inflammatory cascades in the brain.

Methods We used data from the Translational Biomarkers of Alzheimer's Disease (TRIAD) cohort ($n = 137$) to investigate the association between YKL-40, a marker of reactive astrogliosis, and tau burden measured with PET imaging, while also exploring the involvement of APOE ε4 carriership. Statistical analyses included correlation and regression models controlling for age and sex.

Results Here we show that tau pathology is positively associated with YKL-40 levels, reflecting regional patterns of astrocyte activity in the brain. Furthermore, this association is more widespread in individuals carrying the APOE ε4 allele, suggesting a genotype-specific modulation of the glial neuroinflammatory response.

Conclusions Our findings demonstrate a link between tau accumulation and astrocyte-mediated neuroinflammation in AD and highlight the modulatory role of APOE ε4 in this process. Taken together, our findings help inform the multifaceted role of tau-associated neuroinflammation in the progression of AD.

Plain language summary

Alzheimer's disease is a brain disorder characterized by the accumulation of abnormal proteins, including tau, which contribute to memory loss and cognitive decline. Brain support cells called astrocytes respond to this protein build-up by becoming reactive, which can lead to inflammation in the brain. In this study, we used brain scans and cerebrospinal fluid samples from 137 participants to examine how astrocyte reactivity, measured by the protein YKL-40, relates to tau accumulation. We also investigated whether carrying a common genetic risk factor, APOE ε4, influences this relationship. We found that higher tau levels are associated with increased astrocyte reactivity, and this association is stronger in people carrying APOE ε4. These findings suggest that genetic risk may amplify inflammation in Alzheimer's disease.

The pathophysiological hallmarks of Alzheimer's disease (AD) include extracellular amyloid-β plaques and intracellular tangles composed of paired helical filaments of hyperphosphorylated tau^{1,2}. Inflammation and genetic factors, particularly the polymorphism in the apolipoprotein E (APOE) gene, have also been linked to amyloid-β and tau aggregates³. Specifically, the ε4 allele is well recognized to be strongly associated with a higher risk of developing sporadic AD, and is believed to play a role in the underlying mechanisms of AD proteinopathy⁴. For one, APOE

ε4 increases amyloid-β burden, possibly through reduced clearance^{5–7}. Independent from this effect on amyloid-β, APOE ε4 carriership may also lead to increased tau accumulation and tau-mediated neurodegeneration^{8–10}. Importantly, APOE ε4 is associated with inflammatory responses in AD^{11,12}. These observations have led to neuroinflammation gaining recognition as a key factor in AD pathogenesis, with particular interest in how APOE ε4 may exacerbate inflammatory pathways¹¹.

A full list of affiliations appears at the end of the paper. ✉e-mail: lydia.trudel@mail.mcgill.ca; pedro.rosa@mcgill.ca

Astrocytes, an abundant type of glial cells, participate in neuroinflammatory processes^{13–15}. In response to CNS injury or disease, they become abnormally reactive, with the goal of restoring homeostasis by promoting tissue repair and enhancing clearance of debris and metabolic waste products from the brain^{11,16,17}. This response, called reactive astrogliosis, is characterized by morphological, molecular and functional changes, including leakage, release or secretion of proteins¹⁸. Among other proteins, reactive astrocytes overexpress Chitinase-3-like protein 1 (CHI3L1), also named YKL-40, as part of their inflammatory response¹⁸. This observation has been made in patients with MCI and AD dementia, where increased levels of YKL-40 mRNA and elevated CSF levels of YKL-40 are found in the brain^{19–22}. Furthermore, recent meta-analyses report that YKL-40 is consistently elevated in the CSF of individuals with AD²³.

Given that astrocytes are the main producers of the apoE protein in the CNS, the interplay between *APOE* and astrocytic function may be linked to AD proteinopathy²⁴. Specifically, as *APOE* is predominantly expressed in astrocytes, the ε4 allele is believed to alter their normal function, leading to deficient amyloid-β clearance, cerebral hypometabolism and an exacerbated pro-inflammatory response^{25,26}. In addition, studies in mice have shown that the apoE ε4 isoform also disrupts the normal tau clearance process of astrocytes²⁷. Among astrocytic markers, YKL-40 has distinguished itself by showing a specific association with tau pathology compared to others, such as GFAP²⁸. Therefore, this study aimed to assess the relationship between astrocyte reactivity, assessed by cerebrospinal fluid (CSF) YKL-40, and tau burden measured by positron emission tomography (PET) imaging, while also investigating whether *APOE* ε4 carriership influences this relationship.

Here, we show that astrocyte reactivity, measured by CSF YKL-40, is positively associated with tau burden in the brain. Importantly, *APOE* ε4 carriership potentiates this relationship, indicating that genetic risk may exacerbate tau-related neuroinflammatory processes. These findings support a role for astrocyte-mediated inflammation in tau pathology and highlight *APOE* ε4 as a key modulator of this mechanism in AD.

Methods

Participants

Data from this study were obtained from the Translational Biomarkers in Aging and Dementia (TRIAD) cohort. The sample included 132 individuals [22 young individuals, 74 cognitively unimpaired (CU) older adults, 18 with mild cognitive impairment (MCI), 18 with AD dementia]. Each participant underwent structural magnetic resonance imaging (MRI), amyloid-β-PET using [¹⁸F]AZD4694, tau-PET using [¹⁸F]MK6240 and neuropsychological assessments. Cerebrospinal fluid (CSF) concentrations of chitinase-3-like protein 1 (YKL-40) were also measured through lumbar puncture. Comprehensive clinical evaluations were conducted on all subjects. The Clinical Dementia Rating (CDR) was administered to older participants only. Cognitively unimpaired participants had a CDR score of 0, while those with MCI had a CDR of 0.5 and exhibited objective cognitive impairment with relatively preserved activities of daily living performance. AD dementia participants had a CDR of 1 or 2 and met the standard diagnostic criteria for probable AD²⁹. No participants were diagnosed with other neurological or major neuropsychiatric disorders. Individuals with a history of a psychotic disorder, major depressive disorder, substance abuse or autoimmune disease and cancer within two years prior to screening, along with participants with contraindications to PET or MRI, were excluded. The study was conducted in accordance with the Declaration of Helsinki and received approval from the Montreal Neurological Institute PET Working Committee and the Douglas Mental Health University Institute Research Ethics Board. Written informed consent was obtained from all participants.

Fluid biomarkers

All samples were processed and analyzed at the Clinical Neurochemistry Laboratory, University of Gothenburg, Sweden, by scientists blinded to clinical, demographic and biomarker information, as described previously³⁰. Briefly, CSF levels of YKL-40 were quantified using a commercially available ELISA assay (R&D Systems, Minneapolis, MN, USA, catalog #DY2599)³¹.

Neuroimaging

Study participants underwent magnetic resonance imaging (MRI) using 3D T1-weighted sequences on a 3 T Siemens scanner, which facilitated coregistration. In addition, they received [¹⁸F]AZD4694 amyloid-β-PET and [¹⁸F]MK6240 tau-PET scans, both performed with the Siemens High Resolution Research Tomograph (HRRT) at the MNI. The [¹⁸F]AZD4694 images were captured 40–70 min post-injection, reconstructed using the OSEM algorithm on a 4D volume with three frames (3 × 600 s) as described previously³². For [¹⁸F]MK6240, images were acquired 90–110 min post-injection and similarly reconstructed on a 4D volume with four frames (4 × 300 s). Each PET scan was followed by an 11-min transmission scan using a rotating ¹³⁷Cs point source for attenuation correction. The images were adjusted for dead time, decay, and random and scattered coincidences. T1-weighted MRI images were corrected for non-uniformity and field distortions, and then PET images were automatically aligned to the T1-weighted space. The T1-weighted images were subsequently linearly and non-linearly registered to the MNI reference space. PET images underwent meninges and skull stripping, followed by non-linear registration to MNI space using the transformations from T1-weighted to MNI space and from PET to T1-weighted space. The standardized uptake value ratio (SUVR) for [¹⁸F]AZD4694 Aβ-PET used the cerebellum gray matter as the reference region, while for [¹⁸F]MK6240 tau-PET, the inferior cerebellum gray matter served as the reference. Finally, PET images were spatially smoothed to achieve an 8-mm full-width at half-maximum resolution.

Global Aβ PET SUVR was estimated across the prefrontal, orbitofrontal, precuneus, parietal, temporal, and cingulate cortices³³. A composite measure of tau-PET SUVR was calculated within a temporal meta-ROI that includes the entorhinal, parahippocampal, hippocampal, fusiform, inferior temporal, and middle temporal cortices³³. PET Braak-like stages were determined based on brain regions that correspond to the Braak stages of tau tangle accumulation observed postmortem^{34,35} and PET studies^{36–39}. These stages include: Braak I (transentorhinal), Braak II (entorhinal and hippocampus), Braak III (amygdala, fusiform gyrus, parahippocampal gyrus, and lingual gyrus), Braak IV (insula, inferior temporal, lateral temporal, and inferior parietal and posterior cingulate), Braak V (orbitofrontal, inferior frontal, superior frontal, rostromedial frontal, superior temporal, cuneus, precuneus, anterior cingulate, supramarginal gyrus, lateral occipital and superior parietal), and Braak VI (paracentral, precentral, postcentral, and pericalcarine).

We obtained images of the YKL-40 gene expression in the brain from the Allen Human Brain Atlas (www.brain-map.org), a publicly available resource developed by the Allen Institute for Brain Science^{40,41}. Briefly, mRNA expression intensity values were calculated using microarray data from 3702 samples taken from six healthy human postmortem brains (four males, mean age = 42.5 ± 13.4 years, postmortem delay = 20.6 ± 7 h). The YKL-40 mRNA brain expression maps were generated using a Gaussian process⁴² and downloaded from the following website: www.meduniwien.ac.at/neuroimaging/mRNA.html. Brain tissue was collected after obtaining informed consent from donors' next-of-kin. Collection of tissue and associated non-identifying case information was reviewed and approved by the Institutional Review Boards of the tissue banks and repositories that provided material for this project (<http://human.brain-map.org>; see Documentation). Finally, we defined the regions of interest (ROIs) using the DKT atlas (Klein & Tourville, 2012), and we extracted mRNA expression in each of the ROIs.

APOE genotyping

APOE genotyping was performed after blood collection using the TaqMan allelic discrimination assay⁴³.

Statistics and reproducibility

Statistical analyses were performed in R v.2024.04.2, and voxelwise analyses were done using the R Package for Medical Imaging NetCD (MINC) v.1.5.3.0. To assess demographic data, independent-samples *t*-tests were performed, examining differences between CUs and other cognitively

impaired groups for continuous variables. We employed contingency χ^2 tests for categorical variables. We used voxelwise linear regression models to assess the relationship between CSF YKL-40 and tau-PET, correcting for age, sex and global amyloid-PET SUVR. Analyses were repeated in *APOE* ε4 carriership subgroups. A model assessing the interaction between *APOE* ε4 status and CSF YKL-40 was also tested. All voxelwise analyses were corrected for multiple comparisons using random field theory with a threshold of $p < 0.001$. To assess regional colocalization between YKL-40 mRNA expression and the regional association between CSF YKL-40 and tau-PET, we segmented both the t-map and the YKL-40 mRNA expression map using the DKT atlas. We then ran a Spearman correlation analysis between mRNA expression levels and t-values across regions. To extract tau-PET SUVR in regions of significant interaction, we created a mask using the MINC Toolkit (version 1.9.16). All beta coefficients reported in the paper represent standardized beta values. Collinearity was assessed for all variables in the regression models to make sure there was no inflation of coefficients due to collinearity. To do so, we employed the Variance Inflation Factor (VIF), using the car package in R.

Results

Participants

We included 132 individuals from the Translational Biomarkers in Aging and Dementia (TRIAD) cohort [22 young individuals, 74 cognitively unimpaired (CU) older adults, 18 individuals with mild cognitive impairment (MCI), and 18 individuals with dementia] in the study. Following *APOE* genotyping, 50 individuals (37.9%) were identified as *APOE* ε4 carriers, and 82 (62.1%) as *APOE* ε4 non-carriers. Demographic characteristics of the population are listed in Table 1, and demographic characteristics of individuals stratified by *APOE* ε4 carriership are summarized in Supplementary Table 1. Overall, cognitively impaired individuals (individuals with MCI or AD dementia) displayed higher CSF YKL-40 levels than CU and young participants. Additionally, we observed an aging effect, with older CU participants showing higher YKL-40 levels compared to younger individuals (Supplementary Fig. 1).

CSF YKL-40 is associated with tau-PET

First, to assess the relationship between CSF YKL-40 and tau-PET SUVR, we performed a voxelwise regression analysis correcting for age, sex, and global amyloid-PET standardized uptake value ratio (SUVR). Positive associations were found in the precuneus, parietal and temporal lobes and cingulate gyrus (Fig. 1A). Regression analyses controlling for age, sex and global amyloid-PET SUVR were also performed at the ROI level using tau-PET SUVR in the temporal meta-ROI. We found a significant main effect of CSF YKL-40 ($\beta = 0.42$, 95% CI [0.27, 0.58], $p < 0.0001$) (Fig. 1C). Sensitivity analyses excluding the cognitively unimpaired individuals and including only tau-PET-positive individuals yielded similar results (Supplementary Fig. 2). In addition, sensitivity analyses using tau-PET SUVR in Braak stage-

specific ROIs also showed consistent associations between CSF YKL-40 and regional tau burden (Supplementary Fig. 3). Collinearity was assessed for all variables in the model; we obtained a VIF smaller than 2, suggesting no inflation of coefficients due to collinearity.

Association patterns between CSF YKL-40 and tau-PET colocalize with YKL-40 gene expression

We then extracted the topographical map of YKL-40 mRNA expression in six cognitively unimpaired individuals from the Allen Human Brain Atlas (Fig. 1B). Segmentation of the expression map with the Desikan-Killiany-Tourville (DKT) atlas⁴⁴ revealed the highest mRNA expression levels in the precuneus and superior parietal regions (Fig. 1D). Next, to assess regional colocalization, we compared regional YKL-40 mRNA expression with the regional association between tau-PET and CSF YKL-40 as presented in Fig. 1A. Segmentation of the t-map using the DKT atlas allowed for a Spearman correlation analysis between mRNA expression levels and t-values across regions, revealing a significant overlap between regions of association of CSF YKL-40 and tau-PET and regions with high YKL-40 mRNA expression ($r = 0.33$, $p = 0.002$) (Fig. 1E).

CSF YKL-40 is strongly associated with tau-PET in *APOE* ε4 carriers

Next, to assess the involvement of *APOE* ε4 carriership, we performed a voxelwise regression analysis of CSF YKL-40 predicting tau-PET SUVR in the *APOE* ε4 carrier and non-carrier subgroups, controlling for age, sex, and global amyloid-PET SUVR. We found strong significant associations in the precuneus, parietal and temporal lobes only in *APOE* ε4 carriers (Fig. 2A). Sensitivity analyses excluding the cognitively unimpaired individuals yielded similar results (Supplementary Fig. 4). Images showing average tau-PET uptake across the brain for *APOE* ε4 carriers and non-carriers are included in supplementary materials (Supplementary Fig. 5).

We also assessed the voxelwise interaction between *APOE* ε4 carriership and CSF YKL-40 on tau-PET, correcting for age, sex, and global amyloid-PET SUVR. We observed that *APOE* ε4 potentiates the relationship between CSF YKL-40 and tau-PET in the medial temporal lobes, and most strongly in the right hippocampus (Fig. 2B). We extracted tau-PET SUVR values in the region of interaction and corrected them for global amyloid-PET SUVR. We found that after adjusting for global amyloid-PET burden, *APOE* ε4 carriers display significantly more tau in this area, as confirmed by the Wilcoxon rank-sum test ($p < 0.001$) (Fig. 2C). Sensitivity analyses excluding the cognitively unimpaired individuals yielded similar results (Supplementary Fig. 5).

Discussion

In the current study, we aimed to assess the associations between astrocyte reactivity as quantified by CSF YKL-40, *APOE* ε4 carriership and tau deposition in AD. We observed significant associations between tau

Table 1 | Demographics of TRIAD sample

	Young	CU	MCI	p-value	AD dementia	p-value
No.	22	74	18	-	18	-
Age, mean (SD), years	22.5 (1.9)	69.9 (7.6)	72.2 (4.9)	0.12	62.2 (6.1)	6.9×10^{-5}
Male, no. (%)	8 (36)	29 (39)	11 (61)	0.092	10 (56)	0.21
Education, mean (SD), years	16.9 (1.6)	14.8 (3.4)	15.9 (2.9)	0.17	14.3 (2.5)	0.43
<i>APOE</i> ε4 carriers, no. (%)	6 (27)	22 (30)	10 (56)	0.039	12 (67)	0.0036
MMSE, mean (SD)	29.8 (0.53)	29.1 (0.98)	27.9 (2.1)	0.050	21.7 (4.8)	6.1×10^{-6}
CDR SoB, mean (SD)	-	0.05 (0.16)	1.38 (0.86)	8.8×10^{-6}	5.33 (2.8)	4.5×10^{-7}
[¹⁸ F]AZD4694 SUVR, mean (SD)	1.19 (0.066)	1.46 (0.38)	2.32 (0.42)	4.2×10^{-8}	2.29 (0.43)	9.5×10^{-8}
[¹⁸ F]MK6240 SUVR, mean (SD)	0.92 (0.075)	0.98 (0.18)	1.43 (0.50)	0.0016	2.41 (0.85)	1.5×10^{-6}

Independent-samples t-tests (two-sided) were performed to compute comparisons between CU individuals and other cognitively impaired groups for continuous variables. We employed contingency χ^2 tests (two-sided) for *APOE* ε4 status and sex. Values for [¹⁸F]AZD4694 SUVR represent global amyloid-PET SUVR, while [¹⁸F]MK6240 SUVR reflects tau-PET SUVR in the temporal meta-ROI.

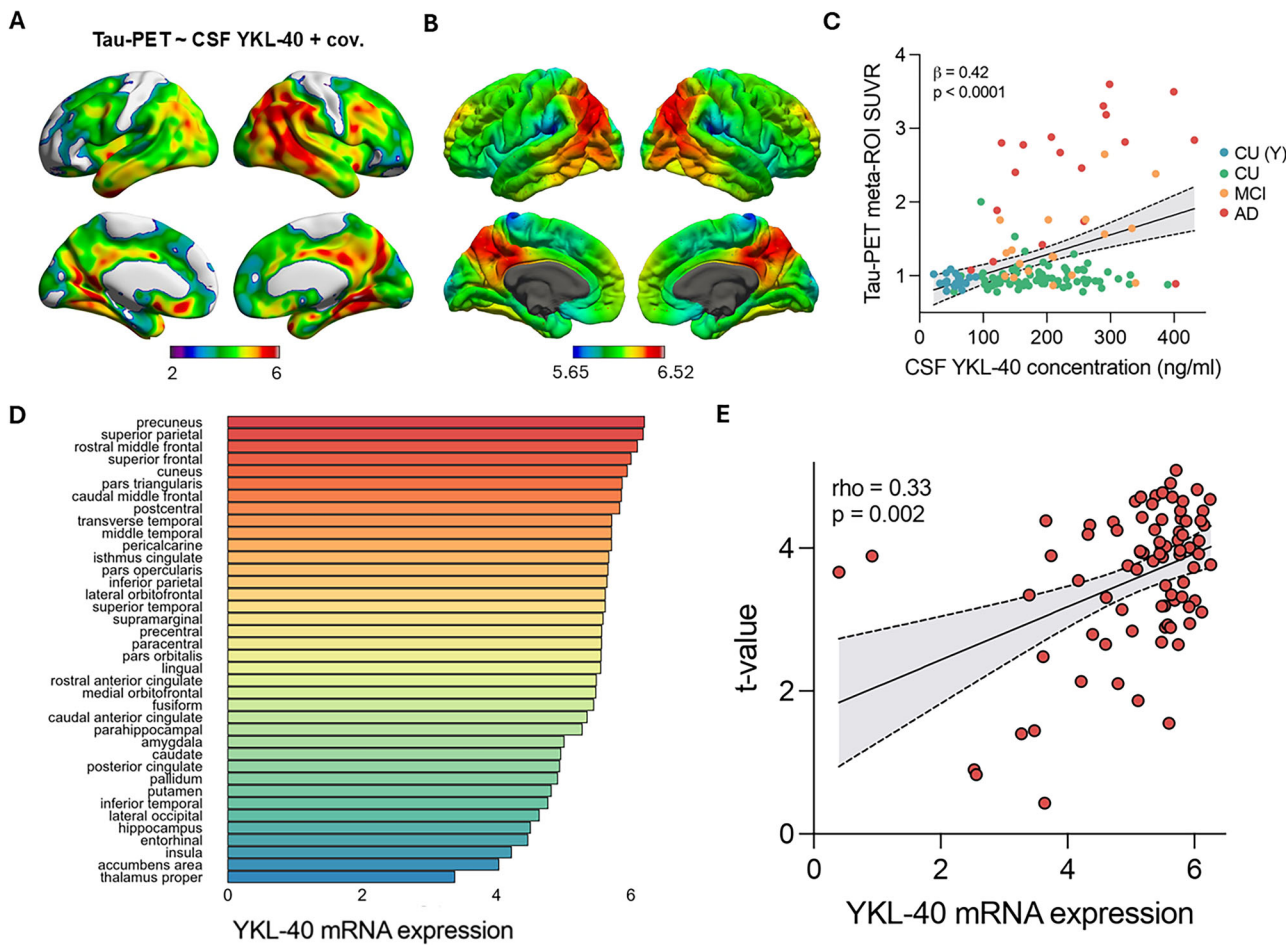


Fig. 1 | Tau-PET is associated with CSF YKL-40 in regions that resemble those of YKL-40 mRNA expression. A Voxelwise linear regression between CSF YKL-40 and tau-PET corrected for age, sex and global amyloid- β (two-sided, RFT corrected at $p < 0.001$). Color bar indicates t-values. B Brain map of the topographical distribution of YKL-40 mRNA expression in six cognitively unimpaired individuals obtained from the Allen Human Brain Atlas. C Association between CSF YKL-40 and meta-ROI tau-PET SUVR across clinical diagnoses. We employed a two-sided

linear regression model controlling for age, sex and amyloid- β . Beta coefficient represents standardized beta value ($p < 2.2 \times 10^{-16}$), $n = 132$ (22 young individuals, 74 CU individuals, 18 individuals with MCI, 18 individuals with AD). D Bars show average mRNA expression in each DKT brain region. E Spearman correlation (two-sided) between YKL-40 mRNA expression and t-value extracted from the association in (A). Each dot represents a different DKT brain region ($n = 38$ regions).

pathology and YKL-40 levels, and these associations were highest in regions of high YKL-40 mRNA expression. When separating individuals into *APOE* $\epsilon 4$ carriers and non-carriers, the association with tau pathology was more widespread in *APOE* $\epsilon 4$ carriers. Furthermore, we found that CSF YKL-40 interacts with *APOE* $\epsilon 4$ status, correlating with greater tau accumulation in the medial temporal lobes. Overall, our findings emphasize the significance of *APOE* $\epsilon 4$ in glial-related neuroinflammation and tau accumulation in AD.

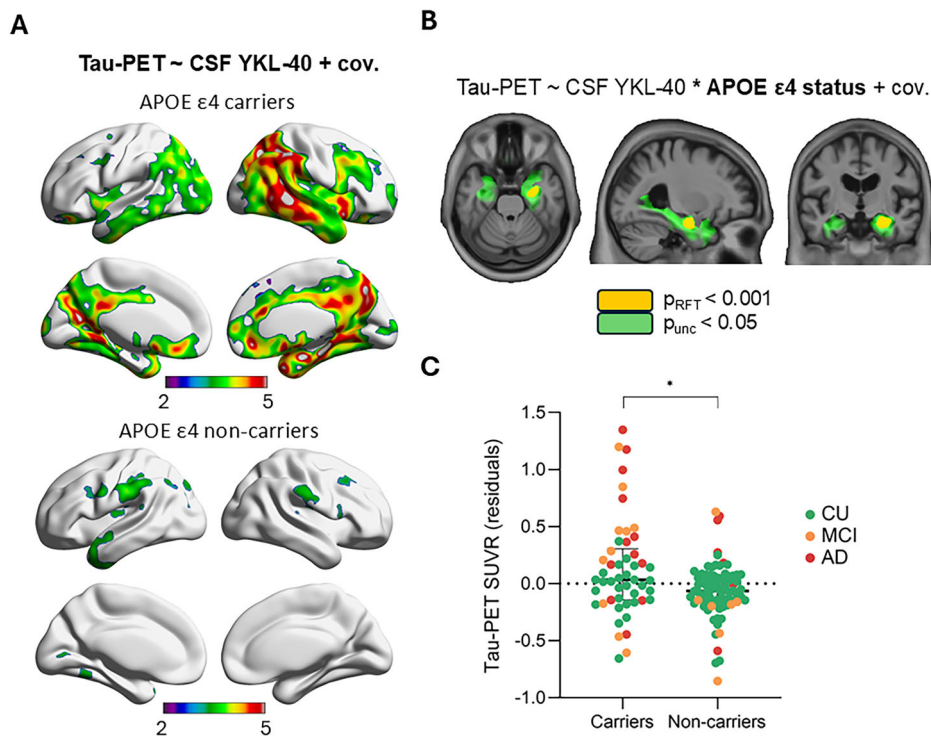
We first demonstrated that there is a significant association between tau burden and YKL-40 levels in the precuneus, middle temporal and posterior temporal cortices. These results corroborate numerous studies showing increased YKL-40 levels in AD, associated with greater tau burden^{28,45–47}. Other studies have also highlighted the role of YKL-40 in amyloid- β -induced tau pathology^{8,48}. Strikingly, the topography of associations between YKL-40 and tau burden followed patterns that resemble those of YKL-40 mRNA expression assessed postmortem. More precisely, using the Allen Brain Atlas, we demonstrated that the magnitude of associations between YKL-40 and tau-PET is highest in regions of high YKL-40 mRNA expression. These results suggest regional contributions of astrocyte reactivity to local tau burden. In addition, the precuneus, middle temporal gyrus and the posterior temporal gyrus are Braak stage IV regions, affected in intermediate stages of AD. These findings also support the idea that YKL-

40 could be a potential biomarker for intermediate tau-related pathology. This notion is further supported by recent findings demonstrating that CSF YKL-40 is strongly associated with tau-PET burden in AD, in contrast to other astrocytic markers such as GFAP, which are more closely related to amyloid- β pathology²⁸.

When separating individuals into *APOE* $\epsilon 4$ carriership subgroups, the association between YKL-40 and tau burden was stronger and more widespread in *APOE* $\epsilon 4$ carriers, suggesting a genotype-specific modulation of the neuroinflammatory response. Studies in rodents have shown that apoE $\epsilon 4$ increases pro-inflammatory astrocytes by epigenetic mechanisms and impairs tau clearance²⁷. A plausible explanation is that *APOE* $\epsilon 4$ promotes astrocytic activation and tau-mediated neurodegeneration through disrupted lipid metabolism and impaired lipid shuttling between astroglia and neurons⁴⁹. Supporting this, a recent study demonstrated that promoting glial lipid efflux attenuates tau pathology, astrogliosis and neurodegeneration in mice⁵⁰. Future work employing fluid biomarkers of cholesterol metabolism and astrogliosis may help evaluate whether similar lipid-mediated mechanisms underlie astrocytic activation and tau accumulation in *APOE* $\epsilon 4$ carriers.

Our analyses also revealed a significant interaction between CSF YKL-40 and *APOE* $\epsilon 4$ status in predicting tau-PET uptake in the hippocampus, a region where *APOE* is highly expressed. A recent study in

Fig. 2 | Tau-PET is strongly associated with CSF YKL-40 in *APOE ε4* carriers. A Voxelwise linear regression between CSF YKL-40 and tau-PET in *APOE ε4* carriers and non-carriers (two-sided, RFT corrected at $p < 0.001$). Color bar indicates t-values. B Voxelwise linear regression model with interaction between CSF YKL-40 and *APOE ε4* status on tau-PET (two-sided) correcting for age, sex and global amyloid- β . Orange shows results of interaction corrected for multiple comparisons ($p < 0.001$), green shows uncorrected results ($p < 0.05$). C Tau-PET SUVR controlling for global amyloid- β in regions of interaction displayed in orange, in *APOE ε4* carriers and non-carriers, $n = 132$ (50 *APOE ε4* carriers, 82 *APOE ε4* non-carriers). Stars show the level of significance of a two-sided Wilcoxon rank-sum test ($p = 0.009$).



mice demonstrated that the removal of neuronal *APOE ε4* reduces both the accumulation of tau pathology and astrogliosis specifically in the hippocampus, highlighting the causal role of neuronal *APOE ε4* in modulating tau-associated astrogliosis⁵¹. Our results in humans complement these findings by suggesting a role of *APOE ε4* in promoting tau-mediated reactive astrogliosis, particularly within medial temporal regions. These results are also in alignment with many studies that have shown that YKL-40 levels are elevated in early stages of the disease^{52,53}. Given that the hippocampus is one of the earliest regions affected by tau pathology, the interaction we observed in this region further supports the role of YKL-40 as an early marker of astrocyte-mediated neuroinflammation in AD.

It is important to note several limitations that warrant discussion. First, YKL-40 is limited by its non-specificity. YKL-40 levels are increased in autoimmune diseases and multiple types of cancer⁵⁴. This non-specificity suggests that while elevated YKL-40 levels in AD may be significant, they could also reflect broader inflammatory processes, which should be considered when interpreting our findings. However, participants with autoimmune disease and cancer within 2 years before participation were excluded from our study. In the same line of thought, while our results support a tau-associated astrocytic response, future studies should evaluate the role of YKL-40 increases in other tauopathies to confirm the specificity of these findings. Furthermore, because we sampled YKL-40 from CSF, the influence of peripheral inflammatory processes on our results is likely negligible. Another limitation of this study is the lack of longitudinal data for CSF YKL-40. Having multiple time points for astrocyte reactivity would refine the analyses and make for stronger conclusions regarding the temporal sequence of events through AD progression. Furthermore, our study sample consists of individuals who are motivated to participate in a study of aging and AD and are potentially not representative of the broader population. Next, our sample size is relatively small, which limits the power of our results. An additional limitation is the age-related increase in CSF YKL-40 levels, which may have contributed to our findings. However, this

influence is likely minimal, as all analyses were adjusted for age. Another limitation is that while *APOE* is a key genetic factor influencing AD risk and related biomarkers, other genetic factors, such as those near the CHI3L1 gene, could also significantly impact astrocyte regulation and CSF YKL-40 levels⁵⁵. Finally, astrocytic reactivity is a dynamic process, during which multiple proteins can rapidly change across disease stages⁵⁶. TSPO-PET, a marker of microglial activation, and fluid biomarker panels assessing broader inflammatory pathways could provide valuable complementary insights into the evolving neuroinflammatory landscape in AD.

In summary, our results contribute to the understanding of glial-related neuroinflammation in AD by evaluating associations between *APOE ε4*, YKL-40 and tau pathology. Our results highlight the importance of neuroinflammation in the pathogenesis of AD, especially in the presence of genetic risk factors such as *APOE ε4*.

Data availability

Source data for the figures can be found in Supplementary Data Files 1–4: The source data for Fig. 1C is in Supplementary Data 1, the source data for Fig. 1D is in Supplementary Data 2, the source data for Fig. 1E is in Supplementary Data 3, and the source data for Fig. 2C is in Supplementary Data 4. Access to analyzed TRIAD cohort data and study materials will be considered by McGill University to ensure compliance with institutional intellectual property and confidentiality policies. Anonymized TRIAD data will be made available by the senior author (Dr. Pedro Rosa-Neto—pedro.rosa@mcgill.ca) to qualified academic investigators for the sole purpose of reproducing the analyses and results reported in this manuscript. Data and materials that can be shared will be released under a material transfer agreement. The Allen Human Brain atlas, including the gene expression data used in this study, can be accessed here without registration: <https://www.meduniwien.ac.at/neuroimaging/mRNA.html>. Users can freely browse and download data directly from the portal.

Received: 10 March 2025; Accepted: 29 September 2025;
Published online: 20 November 2025

References

1. Hyman, B. T. et al. National Institute on Aging-Alzheimer's Association guidelines for the neuropathologic assessment of Alzheimer's disease. *Alzheimers Dement.* **8**, 1–13 (2012).
2. Jack, C. R. Jr. et al. Revised criteria for diagnosis and staging of Alzheimer's disease: Alzheimer's Association Workgroup. *Alzheimers Dement.* **20**, 5143–5169 (2024).
3. Heneka, M. T. et al. Neuroinflammation in Alzheimer's disease. *Lancet Neurol.* **14**, 388–405 (2015).
4. Ayyubova, G. APOE4 is a risk factor and potential therapeutic target for Alzheimer's disease. *CNS Neurol. Disord. Drug Targets* **23**, 342–352 (2024).
5. Castellano, J. M. et al. Human apoE isoforms differentially regulate brain amyloid-beta peptide clearance. *Sci. Transl. Med.* **3**, 89ra57 (2011).
6. Liu, C. C. et al. ApoE4 accelerates early seeding of amyloid pathology. *Neuron* **96**, 1024–1032.e3 (2017).
7. Liu, C. C. et al. Neuronal heparan sulfates promote amyloid pathology by modulating brain amyloid-beta clearance and aggregation in Alzheimer's disease. *Sci. Transl. Med.* **8**, 332ra44 (2016).
8. Ferrari-Souza, J. P. et al. APOE4 potentiates amyloid beta effects on longitudinal tau pathology. *Nat. Aging* **3**, 1210–1218 (2023).
9. Shi, Y. et al. ApoE4 markedly exacerbates tau-mediated neurodegeneration in a mouse model of tauopathy. *Nature* **549**, 523–527 (2017).
10. Therriault, J. et al. Association of apolipoprotein E ϵ 4 with medial temporal tau independent of amyloid-beta. *JAMA Neurol.* **77**, 470–479 (2020).
11. Parhizkar, S. & Holtzman, D. M. APOE mediated neuroinflammation and neurodegeneration in Alzheimer's disease. *Semin. Immunol.* **59**, 101594 (2022).
12. Ferrari-Souza, J. P. et al. APOE ϵ 4 associates with microglial activation independently of A β plaques and tau tangles. *Sci. Adv.* **9**, eade1474 (2023).
13. Colombo, E. & Farina, C. Astrocytes: key regulators of neuroinflammation. *Trends Immunol.* **37**, 608–620 (2016).
14. Gradišnik, L. & Velnar, T. Astrocytes in the central nervous system and their functions in health and disease: a review. *World J. Clin. Cases* **11**, 3385–3394 (2023).
15. Kwon, H. S. & Koh, S. H. Neuroinflammation in neurodegenerative disorders: the roles of microglia and astrocytes. *Transl. Neurodegener.* **9**, 42 (2020).
16. Wyss-Coray, T. Inflammation in Alzheimer disease: driving force, bystander or beneficial response? *Nat. Med.* **12**, 1005–1015 (2006).
17. Wyss-Coray, T. & Mucke, L. Inflammation in neurodegenerative disease—a double-edged sword. *Neuron* **35**, 419–432 (2002).
18. Escartin, C. et al. Reactive astrocyte nomenclature, definitions, and future directions. *Nat. Neurosci.* **24**, 312–325 (2021).
19. Craig-Schapiro, R. et al. YKL-40: a novel prognostic fluid biomarker for preclinical Alzheimer's disease. *Biol. Psychiatry* **68**, 903–912 (2010).
20. Muszynski, P. et al. YKL-40 as a potential biomarker and a possible target in therapeutic strategies of Alzheimer's disease. *Curr. Neuropharmacol.* **15**, 906–917 (2017).
21. Mavroudis, I. et al. YKL-40 as a potential biomarker for the differential diagnosis of Alzheimer's disease. *Medicina* **58**, 60 (2021).
22. Kester, M. I. et al. Cerebrospinal fluid VILIP-1 and YKL-40, candidate biomarkers to diagnose, predict and monitor Alzheimer's disease in a memory clinic cohort. *Alzheimers Res. Ther.* **7**, 59 (2015).
23. Bellaver, B. et al. Astrocyte biomarkers in Alzheimer disease: a systematic review and meta-analysis. *Neurology* **96**, e2944–e2955 (2021).
24. Pitas, R. E. et al. Astrocytes synthesize apolipoprotein E and metabolize apolipoprotein E-containing lipoproteins. *Biochim. Biophys. Acta* **917**, 148–161 (1987).
25. Blumenfeld, J. et al. Cell type-specific roles of APOE4 in Alzheimer disease. *Nat. Rev. Neurosci.* **25**, 91–110 (2024).
26. Fernandez, C. G. et al. The role of APOE4 in disrupting the homeostatic functions of astrocytes and microglia in aging and Alzheimer's disease. *Front. Aging Neurosci.* **11**, 14 (2019).
27. Eisenbaum, M. et al. ApoE4 expression disrupts tau uptake, trafficking, and clearance in astrocytes. *Glia* **72**, 184–205 (2024).
28. Ferrari-Souza, J. P. et al. Astrocyte biomarker signatures of amyloid-beta and tau pathologies in Alzheimer's disease. *Mol. Psychiatry* **27**, 4781–4789 (2022).
29. McKhann, G. M. et al. The diagnosis of dementia due to Alzheimer's disease: recommendations from the National Institute on Aging-Alzheimer's Association workgroups on diagnostic guidelines for Alzheimer's disease. *Alzheimers Dement.* **7**, 263–269 (2011).
30. Benedet, A. L. et al. Differences between plasma and cerebrospinal fluid glial fibrillary acidic protein levels across the Alzheimer disease continuum. *JAMA Neurol.* **78**, 1471–1483 (2021).
31. Jensen, C. S. et al. Exercise as a potential modulator of inflammation in patients with Alzheimer's disease measured in cerebrospinal fluid and plasma. *Exp. Gerontol.* **121**, 91–98 (2019).
32. Pomilio, A. B., Vitale, A. A. & Lazarowski, A. J. Neuroproteomics chip-based mass spectrometry and other techniques for Alzheimer's disease biomarkers—update. *Curr. Pharm. Des.* **28**, 1124–1151 (2022).
33. Jack, C. R. Jr. et al. Defining imaging biomarker cut points for brain aging and Alzheimer's disease. *Alzheimers Dement.* **13**, 205–216 (2017).
34. Braak, H. & Braak, E. Neuropathological stageing of Alzheimer-related changes. *Acta Neuropathol.* **82**, 239–259 (1991).
35. Braak, H. & Braak, E. Frequency of stages of Alzheimer-related lesions in different age categories. *Neurobiol. Aging* **18**, 351–357 (1997).
36. Pascoal, T. A. et al. 18F-MK-6240 PET for early and late detection of neurofibrillary tangles. *Brain* **143**, 2818–2830 (2020).
37. Scholl, M. et al. PET imaging of tau deposition in the aging human brain. *Neuron* **89**, 971–982 (2016).
38. Trudel, L. et al. Implication for clinical trials from longitudinal tau-PET accumulation across biological Alzheimer's disease stages. *Neurology* **105**, e214111 (2025).
39. Trudel, L., Macedo, T. J., Servaes, A. & Hosseini, S. S. A. Rates of clinical progression according to biological Alzheimer's disease stages. *Alzheimers Dement.* **21**, e70624 (2025).
40. Hawrylycz, M. J. et al. An anatomically comprehensive atlas of the adult human brain transcriptome. *Nature* **489**, 391–399 (2012).
41. Sunkin, S. M. et al. Allen Brain Atlas: an integrated spatio-temporal portal for exploring the central nervous system. *Nucleic Acids Res.* **41**, D996–D1008 (2013).
42. Gorylewski, G. et al. Spatial analysis and high resolution mapping of the human whole-brain transcriptome for integrative analysis in neuroimaging. *Neuroimage* **176**, 259–267 (2018).
43. Hixson, J. E. & Vernier, D. T. Restriction isotyping of human apolipoprotein E by gene amplification and cleavage with Hhal. *J. Lipid Res.* **31**, 545–548 (1990).
44. Klein, A. & Tourville, J. 101 labeled brain images and a consistent human cortical labeling protocol. *Front. Neurosci.* **6**, 171 (2012).
45. Baldacci, F. et al. Diagnostic function of the neuroinflammatory biomarker YKL-40 in Alzheimer's disease and other neurodegenerative diseases. *Expert Rev. Proteomics* **14**, 285–299 (2017).
46. Janelidze, S. et al. Cerebrospinal fluid neurogranin and YKL-40 as biomarkers of Alzheimer's disease. *Ann. Clin. Transl. Neurol.* **3**, 12–20 (2016).

47. Wilczynska, K. et al. Serum amyloid biomarkers, tau protein and YKL-40 utility in detection, differential diagnosing, and monitoring of dementia. *Front. Psychiatry* **12**, 725511 (2021).
48. Pelkmans, W. et al. Astrocyte biomarkers GFAP and YKL-40 mediate early Alzheimer's disease progression. *Alzheimers Dement.* **20**, 483–493 (2024).
49. Lee, H. et al. ApoE4-dependent lysosomal cholesterol accumulation impairs mitochondrial homeostasis and oxidative phosphorylation in human astrocytes. *Cell Rep.* **42**, 113183 (2023).
50. Litvinchuk, A. et al. Amelioration of Tau and ApoE4-linked glial lipid accumulation and neurodegeneration with an LXR agonist. *Neuron* **112**, 384–403.e8 (2024).
51. Koutsodendris, N. et al. Neuronal APOE4 removal protects against tau-mediated gliosis, neurodegeneration and myelin deficits. *Nat. Aging* **3**, 275–296 (2023).
52. Janelidze, S. et al. CSF biomarkers of neuroinflammation and cerebrovascular dysfunction in early Alzheimer disease. *Neurology* **91**, e867–e877 (2018).
53. Johnson, E. C. B. et al. Cerebrospinal fluid proteomics define the natural history of autosomal dominant Alzheimer's disease. *Nat. Med.* **29**, 1979–1988 (2023).
54. Yeo, I. J. et al. Roles of chitinase 3-like 1 in the development of cancer, neurodegenerative diseases, and inflammatory diseases. *Pharm. Ther.* **203**, 107394 (2019).
55. Deming, Y. et al. Chitinase-3-like 1 protein (CHI3L1) locus influences cerebrospinal fluid levels of YKL-40. *BMC Neurol.* **16**, 217 (2016).
56. Carter, S. F. et al. Astrocyte biomarkers in Alzheimer's disease. *Trends Mol. Med.* **25**, 77–95 (2019).

Acknowledgements

This research is supported by the Weston Brain Institute, Canadian Institutes of Health Research (CIHR) [MOP-11-51-31; RFN 152985, 159815, 162303], Canadian Consortium of Neurodegeneration and Aging (CCNA; MOP-11-51-31 -team 1), the Alzheimer's Association [NIRG-12-92090, NIRP-12-259245], Brain Canada Foundation (CFI Project 34874; 33397), the Fonds de Recherche du Québec – Santé (FRQS; Chercheur Boursier, 2020-VICO-279314; 2024-VICO-356138). T.A.P., P.R.-N. and S.G. are members of the CIHR-CCNA Canadian Consortium of Neurodegeneration in Aging. H.Z. is a Wallenberg Scholar and a Distinguished Professor at the Swedish Research Council supported by grants from the Swedish Research Council (#2023-00356, #2022-01018 and #2019-02397), the European Union's Horizon Europe research and innovation programme under grant agreement No 101053962, and Swedish State Support for Clinical Research (#ALFGBG-71320). M.M. is funded by Fonds de Recherche du Québec - Chercheur boursier Junior 1.

Authors contributions

L.T., J.T., and P.R.-N. conceptualized and designed the study. L.T. and J.T. performed image processing and ran analyses. J.S. and N.R. coordinated the study enrollment, follow-up, sample collection, and imaging and clinical data acquisition. L.T. wrote the first draft of the manuscript. K.B., H.Z., N.J.A., T.K.K., and A.L.B. were responsible for the analysis of samples and provided critical revision of the manuscript for intellectual content. A.C.M., M.S.W., É.A., S.S., S.A.H., J.P.F.-S., B.B., P.L.-F., T.C., Y.-T.W., J.F.-A., Y.Z., B.H., R.H., C.H.-H.H., M.M., J.K., Y.I.-M., P.V., E.Z., S.G., T.A.P., H.Z., K.B., and P.R.-N. contributed to data interpretation and manuscript review. All authors reviewed and approved the final manuscript.

Competing interests

J.T. has served as a consultant for the Neurotorium Educational Platform and as a medical writer for Alzheon Inc., both outside of the scope of the present work. P.V. serves on the scientific advisory boards for NovoNordisc, Eisai,

and Lilly, and received honoraria from IntelGenx Corp. S.G. is a member of the scientific advisory boards of AbbVie, Alzheon, AmyriAD, Eisai Canada, Enigma USA, Lilly Canada, Novo Nordisk Canada, TauRx. T.C. has served on the scientific advisory board of Eisai outside the scope of the present work. T.K.K. has consulted for Quanterix Corporation, SpearBio Inc., Neurogen Biomarketing LLC., and Alzheon, and has served on advisory boards for Siemens Healthineers and Neurogen Biomarketing LLC., outside the submitted work. He has received in-kind research support from Janssen Research Laboratories, SpearBio Inc., and Alamar Biosciences, as well as meeting travel support from the Alzheimer's Association and Neurogen Biomarketing LLC., outside the submitted work. T.K.K. has received royalties from Bioventix for the transfer of specific antibodies and assays to third-party organizations. He has received honoraria for speaker/grant review engagements from the NIH, UPENN, UW-Madison, the Cherry Blossom symposium, the HABS-HD/ADNI4 Health Enhancement Scientific Program, Advent Health Translational Research Institute, Brain Health conference, Barcelona-Pittsburgh conference, the International Neuropsychological Society, the Icahn School of Medicine at Mount Sinai and the Quebec Center for Drug Discovery, Canada, all outside of the submitted work. T.K.K. is an inventor on several patents and provisional patents regarding biofluid biomarker methods, targets and reagents/compositions, that may generate income for the institution and/or self should they be licensed and/or transferred to another organization. These include WO2020193500A1: Use of a ps396 assay to diagnose tauopathies; US 63/679,361: Methods to Evaluate Early-Stage Pre-Tangle TAU Aggregates and Treatment of Alzheimer's Disease Patients; US 63/672,952: Method for the Quantification of Plasma Amyloid-Beta Biomarkers in Alzheimer's Disease; US 63/693,956: Anti-tau Protein Antigen Binding Reagents; and 2450702-2: Detection of oligomeric tau and soluble tau aggregates. N.J.A. has given lectures in symposia sponsored by Eli-Lilly, Roche Diagnostics, Alamar Biosciences, Biogen, VJDementia and Quanterix; consulted for Quanterix, TauRx, Neurogen Biomarketing; served on advisory boards for Biogen, TauRx, and TargetALS; and has a pending patent application (PCT/US2024/037834 (WSGR Docket No. 58484-709.601): Methods for Remote Blood Collection, Extraction and Analysis of Neuro Biomarkers). E.R.Z. has served on the scientific advisory board, as a consultant or speaker for Nintx, Novo Nordisk, Biogen, Lilly and Magdalena Biosciences. He is also a co-founder and minority shareholder of Masima. H.Z. has served at scientific advisory boards and/or as a consultant for Abbvie, Acumen, Alector, Alzinova, ALZpath, Amylyx, Annexon, Apellis, Artery Therapeutics, AZTherapies, Cognito Therapeutics, CogRx, Denali, Eisai, Enigma, LabCorp, Merck Sharp & Dohme, Merry Life, Nervgen, Novo Nordisk, Optoceutics, Passage Bio, Pinteon Therapeutics, Prothena, Quanterix, Red Abbey Labs, reMYND, Roche, Samumed, ScandiBio Therapeutics AB, Siemens Healthineers, Triplet Therapeutics, and Wave, has given lectures sponsored by Alzecure, BioArctic, Biogen, Cellecrichton, Fujirebio, LabCorp, Lilly, Novo Nordisk, Oy Medix Biochemica AB, Roche, and WebMD, is a co-founder of Brain Biomarker Solutions in Gothenburg AB (BBS), which is a part of the GU Ventures Incubator Program, and is a shareholder of CERimmune Therapeutics (outside submitted work). K.B. has served as a consultant and on advisory boards for AbbVie, AC Immune, ALZPath, AriBio, Beckman-Coulter, BioArctic, Biogen, Eisai, Lilly, Moleac Pte. Ltd, Neurimmune, Novartis, Ono Pharma, Prothena, Quanterix, Roche Diagnostics, Sunbird Bio, Sanofi and Siemens Healthineers; has served at data monitoring committees for Julius Clinical and Novartis; has given lectures, produced educational materials and participated in educational programs for AC Immune, Biogen, Celdara Medical, Eisai and Roche Diagnostics; and is a co-founder of Brain Biomarker Solutions in Gothenburg AB (BBS), which is a part of the GU Ventures Incubator Program, outside the work presented in this paper. P.R.-N. has served on scientific advisory boards and/or as a consultant for Roche, Novo Nordisk, Eisai and Cerveau Technologies, outside of the scope of the present work. All other authors (L.T., A.C.M., N.R., É.A., S.S., S.A.H., J.P.F.-Z., B.B., P.L.F., Y.-T.W., J.F.-A., Y.Z., B.H., J.S., R.H., C.H.H., M.M., J.K. and T.A.P.) declare no competing interests.

Additional information

Supplementary information The online version contains supplementary material available at <https://doi.org/10.1038/s43856-025-01171-4>.

Correspondence and requests for materials should be addressed to Lydia Trudel or Pedro Rosa-Neto.

Peer review information *Communications Medicine* thanks Pablo Botella Lucena, Nobuyuki Okamura, Kristin R. Wildsmith and the other anonymous reviewer(s) for their contribution to the peer review of this work.

Reprints and permissions information is available at <http://www.nature.com/reprints>

Publisher's note Springer Nature remains neutral with regard to jurisdictional claims in published maps and institutional affiliations.

Open Access This article is licensed under a Creative Commons Attribution-NonCommercial-NoDerivatives 4.0 International License, which permits any non-commercial use, sharing, distribution and reproduction in any medium or format, as long as you give appropriate credit to the original author(s) and the source, provide a link to the Creative Commons licence, and indicate if you modified the licensed material. You do not have permission under this licence to share adapted material derived from this article or parts of it. The images or other third party material in this article are included in the article's Creative Commons licence, unless indicated otherwise in a credit line to the material. If material is not included in the article's Creative Commons licence and your intended use is not permitted by statutory regulation or exceeds the permitted use, you will need to obtain permission directly from the copyright holder. To view a copy of this licence, visit <http://creativecommons.org/licenses/by-nc-nd/4.0/>.

© The Author(s) 2025

¹Translational Neuroimaging Laboratory Department of Neurology and Neurosurgery, McConnell Brain Imaging Centre, Montreal Neurological Institute, McGill University, Montreal, QC, Canada. ²McGill University Research Centre for Studies in Aging, Douglas Hospital Research Centre - Centre intégré universitaire de santé et services sociaux de l'Outre-de-l'Île-de-Montréal, Montreal, QC, Canada. ³Department of Neurology and Neurosurgery, Faculty of Medicine, McGill University, Montreal, QC, Canada. ⁴Translational Neurodegeneration Laboratory, Department of Neurology, University Medical Center Hamburg-Eppendorf, Hamburg, Germany. ⁵Institute of Neuroimmunology and Multiple Sclerosis, University Medical Center Hamburg-Eppendorf, Hamburg, Germany. ⁶Department of Psychiatry, School of Medicine, University of Pittsburgh, Pittsburgh, PA, USA. ⁷Graduate Program in Biological Sciences: Biochemistry, Universidade Federal do Rio Grande do Sul, Porto Alegre, Brazil. ⁸PET Unit, McConnell Brain Imaging Centre, Montréal, QC, Canada. ⁹Department of Diagnostic Radiology, Faculty of Medicine, McGill University, Montreal, QC, Canada. ¹⁰Department of Psychiatry and Neurochemistry, Institute of Neuroscience and Physiology, The Sahlgrenska Academy, University of Gothenburg, Mölndal, Sweden. ¹¹King's College London, Institute of Psychiatry, Psychology and Neuroscience, Maurice Wohl Institute Clinical Neuroscience Institute, London, UK. ¹²Clinical Neurochemistry Laboratory, Sahlgrenska University Hospital, Gothenburg, Sweden. ¹³NIHR Biomedical Research Centre for Mental Health and Biomedical Research Unit for Dementia at South London and Maudsley NHS Foundation, London, UK. ¹⁴Centre for Molecular Medicine, University Hospital, Stavanger, Norway. ¹⁵Department of Pharmacology, Universidade Federal do Rio Grande do Sul, Porto Alegre, Brazil. ¹⁶Graduate Program in Biological Sciences: Pharmacology and Therapeutics, Universidade Federal do Rio Grande do Sul, Porto Alegre, Brazil. ¹⁷Department of Neurodegenerative Disease, UCL Queen Square Institute of Neurology, London, UK. ¹⁸UK Dementia Research Institute at UCL, London, UK. ¹⁹Hong Kong Center for Neurodegenerative Diseases, Hong Kong, China. ²⁰Wisconsin Alzheimer's Disease Research Center, University of Wisconsin School of Medicine and Public Health, University of Wisconsin-Madison, Madison, WI, USA. ²¹Paris Brain Institute, ICM, Pitie-Salpêtrière Hospital, Sorbonne University, Paris, France. ²²Neurodegenerative Disorder Research Center, Division of Life Sciences and Medicine, and Department of Neurology, Institute on Aging and Brain Disorders, University of Science and Technology of China and First Affiliated Hospital of USTC, Hefei, P.R. China. ²³Peter O'Donnell Jr. Brain Institute (OBI), University of Texas Southwestern Medical Centre (UTSW), Dallas, Texas, USA.

✉ e-mail: lydia.trudel@mail.mcgill.ca; pedro.rosa@mcgill.ca